View Article Online / Journal Homepage / Table of Contents for this issue

Anodic oxidation of indenofluorene. Electrodeposition of electroactive poly(indenofluorene)†

Joëlle Rault-Berthelot,*[a] Cyril Poriel,[a] Frédéric Justaud[b] and Frédéric Barrière[a]

Received (in Montpellier, France) 3rd January 2008, Accepted 13th March 2008
First published as an Advance Article on the web 23rd April 2008
DOI: 10.1039/b719467f

Poly(indenofluorene) was electrochemically deposited onto anode surfaces in CH_2Cl_2 medium along indenofluorene oxidation. The resulting films were characterized and compared with polyfluorenes. A mechanism of polymerization is proposed in the light of cyclic voltammetry experiments and theoretical calculations.

Published on 23 April 2008 on http://pubs.rsc.org | doi:10.1039/B719467F
Downloaded by University of Belgrade on 01 January 2013

1 Introduction

Luminescent conjugated polymers are of considerable importance as active materials in organic light-emitting diodes (OLED)s.[1] One area of major ongoing effort in academic and industrial research into these materials is the development of materials which show efficient and stable blue emission. In this context, phenylene-based materials *i.e.* polyfluorenes (**PF**s), poly(indenofluorene) (**PIF**s) and ladder-type polyphenylenes (**LPPP**s) are one of the most studied classes of conjugated polymers for electronic applications.[2] These materials show blue to blue–green emission in solution, but in the solid state the appearance of longer wavelength emission causes the emission color to become green or even yellow. The source of this long wavelength emission was initially attributed to excimer emission from aggregates formed by π-stacking of the polymer chains[3,4] and later to the emission from ketonic defects such as 9-fluorenone units incorporated in the polymer backbone.[5–7] In order to suppress the possibility of ketonic defect formation and to decrease the ability of π-stacking, we recently designed new chromophores for blue OLED applications.[8,9] These compounds called DiSpiro-Fluorene-IndenoFluorenes (**DSF-IF**s) combine indenofluorene (**IF**) and spirobifluorene (**SBF**) architectural specificities, both known to highly enhance the OLED efficiencies.[10–12]

The development of this new class of luminophores led us to prepare different substituted **DSF-IF** families (Scheme 1). In class I, the spiro-linked fluorenes are not substituted on the 2 and 7 carbon atoms. In this case, anodic oxidation at high potential values leads to deposition on the electrode surface of highly conjugated materials.[8,9] Comparison of the electrochemical properties of these materials and our previous works on fluorene[13–15] and on **SBF** polymerization[16] allows to conclude that anodic oxidation leads to carbon–carbon coupling involving the fluorene units at the classical 2, 7, 2′ and 7′ carbon atoms.

Surprisingly, we recently noticed that in the class II compounds, where the positions 2, 2′, 7 and 7′ of the fluorene carbon rings are blocked (*e.g.* alkyl groups), a polymerization process of rather low yield can also be observed above 1.9 V.[17] These unexpected observations hint to the involvement of the indenofluorene core of class II **DSF-IF**s in the polymerization process (Scheme 2).

For the last ten years, numerous papers have reported different polyindenofluorenes as potential blue emitters for OLED applications: ladder type polyphenylenes,[18] polyindenofluorenes linked through their 6 and 12 carbon atoms,[19–21] ladder type oligo(*p*-phenylene) tethered to a poly(alkylene)

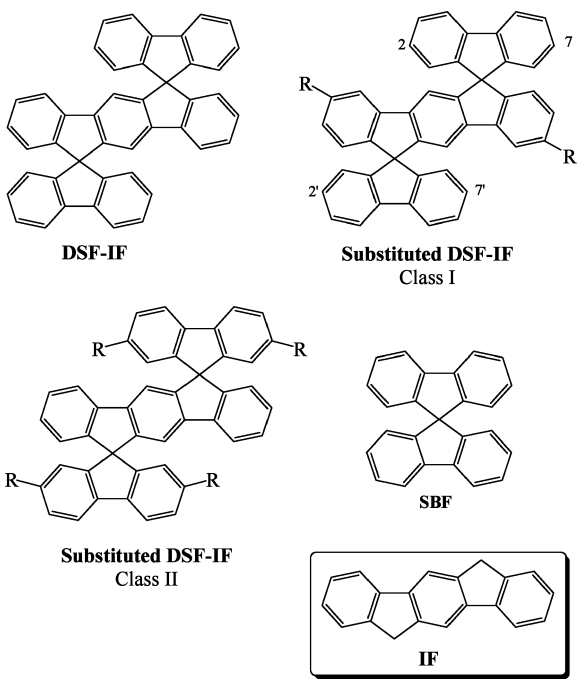

Scheme 1 Structures of **DSF-IF**, **SBF** and **IF** derivatives.

[a] *Université de Rennes 1, CNRS UMR no 6226, Laboratoire de Sciences Chimiques de Rennes, Equipe Matière Condensée et Systèmes Electroactifs, Campus de Beaulieu, Bat. 10C, Avenue du Général Leclerc, 35042 Rennes Cédex, France. E-mail: Joelle.Rault-Berthelot@univ-rennes1.fr; Fax: +332 23 23 67 32; Tel: +332 23 23 59 64*
[b] *Université de Rennes 1, CNRS UMR no 6226, Laboratoire de Sciences Chimiques de Rennes, Equipe OM2, Campus de Beaulieu, Bat. 10C, Avenue du Général Leclerc, 35042 Rennes Cédex, France*

† Electronic supplementary information (ESI) available: Fig. S1: UV-Vis spectrum of the 2,7-(*t*-Bu)$_2$-fluorene radical cation obtained along an *in situ* anodic oxidation of a solution of 2,7-(*t*-Bu)$_2$-fluorene in CH_2Cl_2–Bu_4NPF_6 0.2 M at 1.6 V *vs.* Fc/Fc^+. Fig. S2: ESR spectrum of 2,7-(*t*-Bu)$_2$-fluorene radical recorded at 1.6 V. See DOI: 10.1039/b719467f

View Article Online

Downloaded by University of Belgrade on 01 January 2013
Published on 23 April 2008 on http://pubs.rsc.org | doi:10.1039/B719467F

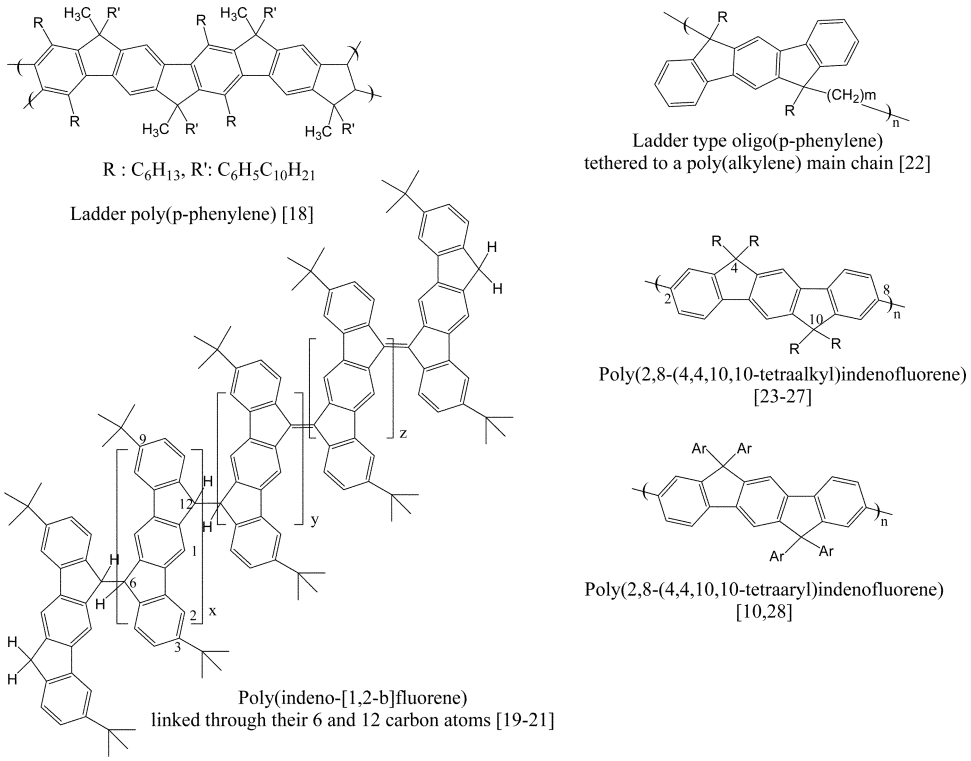

Scheme 2 Structures of polyindenofluorenes described in literature.

main chain[22] or poly(2,8-indenofluorenes) substituted by aryl[23–27] or alkyl groups.[10,28] All these polymers were prepared through chemical routes.

To the best of our knowledge, neither the literature, nor our previous studies on the **IF** anodic oxidation in CH_3CN–CH_2Cl_2 mixed solutions showed any electrodeposition processes of poly(**IF**), so we did not expect electrodeposition for the substituted **DSF-IF**s of class II. Considering the current importance of **IF** materials in optoelectronic, we decided to revisit the anodic oxidation of **IF**. We report herein, the anodic oxidation of **IF** in dichloromethane solution and the electro- and physico-chemical behaviour of the corresponding polymers.

Results and discussion

Monomer anodic oxidation

The electrochemical properties of **IF** (2×10^{-3} M) have been evaluated in CH_2Cl_2 (Bu_4NPF_6 0.2 M) using cyclic voltammetry. Application of a single potential scan between 0.0 and 1.15 V shows one reversible peak E^1 (with maximum at 0.9 V) corresponding to the reversible oxidation of **IF** to its radical cation (Fig. 1(B)). When scanning to 1.9 V, this first wave is followed by a second irreversible one E^2 (with maximum at 1.6 V) of about twice its amplitude (Fig. 1(A)). Fig. 1(C) shows the cyclic voltammograms resulting from the application of repeated potential scans between −0.2 and 1.73 V. This leads to the gradual increase of two new broad redox waves **Ian/Icat** and **IIan/IIcat**, in the 0.35–0.8 and 1.0–1.5 V region respectively, corresponding to the electrodeposition of an electroactive material on the anode surface.

A shift of 0.45 V between **IF** and poly(**IF**) onset potentials is observed (Fig. 1(C)), clearly indicating the extension of

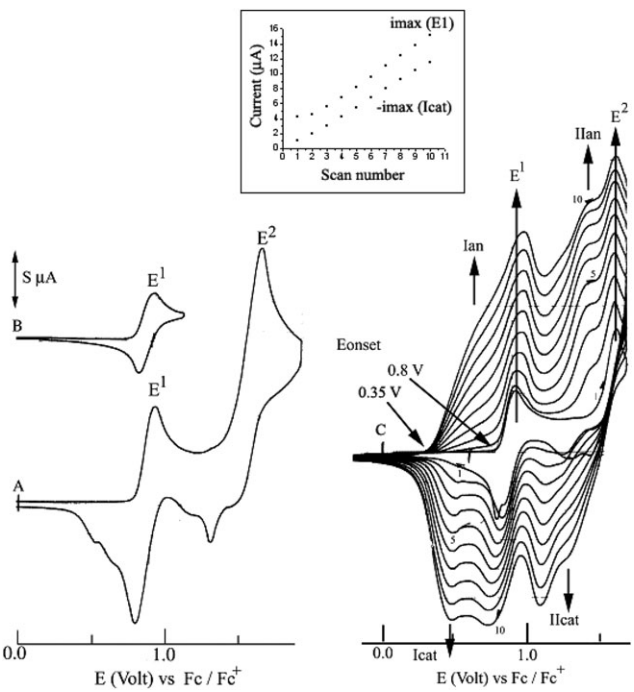

Fig. 1 Cyclic voltammetry in presence of **IF** (2×10^{-3} M) (A–C) in CH_2Cl_2 (Bu_4NPF_6 0.2 M); working electrode: Pt disk diameter 1 mm; sweep-rate 100 mV s^{-1}. The potential limit was of 0.0 to 1.75 V in A; 0.0 to 1.0 V in B; −0.2 to 1.73 V in C. The current scale S is equal to 2 in (A) and to 4 in (B) and in (C). Inset reports the I_{max} at E^1 and $-I_{max}$ at I_{cat} *vs.* the scan number.

 This journal is © The Royal Society of Chemistry and the Centre National de la Recherche Scientifique 2008

Published on 23 April 2008 on http://pubs.rsc.org | doi:10.1039/B719467F
Downloaded by University of Belgrade on 01 January 2013

conjugation in the polymer. Fig. 1(C) shows also the electrodeposition process with a regular increase of the monomer oxidation waves. The inset shows the value of current at E^1 ($i_{max}(E^1)$) and at I_{cat} ($-i_{max}(I_{cat})$) recorded during the 10 scans in Fig. 1(C) *vs.* the scan number and demonstrates the regular increase of the current at each cycle. **IF** has also been electropolymerized under potentiostatic conditions at an applied potential close to E^2.

Microgravimetric quartz-crystal-microbalance analysis

We used a quartz/platinum working electrode to prepare samples of poly(**IF**) of different thickness controlled by the amount of charge, Qt, consumed during the electrodeposition process. The measurement of the quartz crystal frequency before and after the electrodeposition allowed, *via* the Sauerbrey equation,[29] the determination of the mass deposited on the electrode. As shown in Scheme 3, the electrodeposition occurs after consumption of three electrons (one at potential E^1 leading to $\mathbf{IF}^{\bullet +}$ and two at potential E^2 where the electrodeposition process occurs). As soon as the polymer is obtained in its conducting p-doped form, one may add to the three first electrons a charge x of about 0.3–1 electron per **IF** unit corresponding to an average p-doping of the polymer. Consequently, $Qt = (3 + x)nF$, where n is the number of **IF** units involved in the polymer and $F = 96500$ C. The theoretical mass deposit is then the product of n with the molar mass of the indenofluorene unit in the deposit (252 g mol^{-1}). Thus, the **IF** electropolymerization yield is around 45% for the thin deposit and drops to 35% for thicker ones because of limited monomer diffusion (electrodepositions were carried out in quiescent solutions) (Table 1).

Electrochemistry of poly(IF) deposits

In order to obtain deeper insights on the electroactivity and electrochemical stability of the poly(**IF**) deposits, their electrochemical behaviour was studied in monomer-free electrolytic medium. For this purpose, electrodeposition of poly(**IF**) was performed during recurrent CVs or by oxidation at fixed potential followed by the reduction of the deposit at 0.0 V. The modified electrode was then rinsed in CH_2Cl_2 and transferred to an electrolytic solution free of **IF**. As shown in Fig. 2, with a platinum electrode modified after the CV shown in

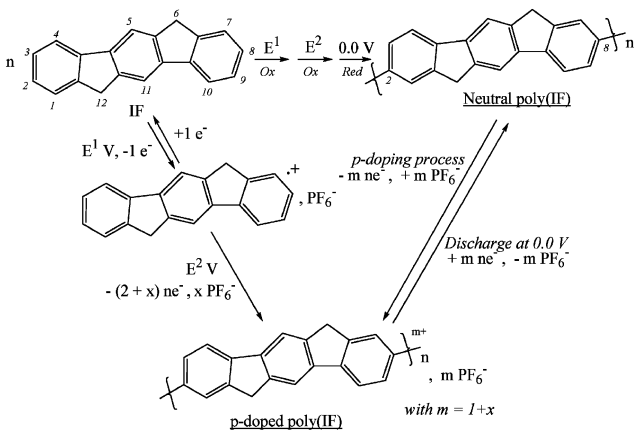

Scheme 3 Anodic polymerization process proposed for **IF** oxidation.

Table 1 Electrodeposition yield determination from coulometric data and deposit mass

Qt/C	Experimental mass deposit/ μg	Theoretical mass deposit/ μg	Electrodeposition yield (%)
2.2×10^{-2}	6.6	17–14	39–47
4.0×10^{-2}	9.9	32–26	31–38

Fig. 1(C), the CV of poly(**IF**) shows two broad anodic waves **Ian** and **IIan** with maxima at 0.84 and 1.20 V, respectively.

The calculation of $100(Q_{red}/Q_{ox})$ (Q_{red} and Q_{ox}: amount of charge consumed during the cathodic and the anodic sweeps) leads to the degree of reversibility of the p-doping process. The reversibility is quantitative for **Ian/Icat** and about 80% for **IIan**/**IIcat**. The third **IIIan**/**IIIcat** wave, with maximum about 1.55 V, has a reversibility of less than 70% and recurrent sweeps between 0.0 and 1.64 V lead to a gradual decrease of the current, corresponding to the gradual overoxidation of the deposit. Poly(**IF**) appears then highly electroactive between 0.35 and 1.36 V while poly(**F**) presents a reversible p-doping process **Ian /Icat** between 0.56 and 1.1 V and a less reversible **IIan/IIcat** process between 1.1 and 1.4 V.[30] The shift of 210 mV between the threshold oxidation potential of poly(**IF**) and poly(**F**) points to a higher conjugation length, which can be first explained by the more extended planarity of the **IF** unit.

In addition, theoretical calculations (density functional theory at the B3LYP/6-31G* level) on two simple oligomeric models (an indenofluorene dimer **di-IF** (40 carbon atoms) and a fluorene trimer **tri-F** (39 carbon atoms)) have been carried out since they have identical length and a similar number of carbon atoms: (Fig. 3). The length of the molecules measured after full geometry optimization of both models is 23.4 Å between the end carbon atoms. Several rotamers are equally stable for both models with quasi-identical calculated absolute energy. The dihedral angles measured between two consecutive indenofluorene moieties (36.8–37.2°) or two fluorene moities (37.0–37.4°) are very similar in these two molecules and among their respective rotamers. However, one of the **tri-F** isomers shows a helical-like rather than a sheet-like twist, so that, on average, the structure of the poly(**F**) polymer is further from an extended planarity than the poly(**IF**). The more conjugated property of poly(**IF**) with respect to poly(**F**) is therefore not only attributed to its longer monomeric planar unit, but also to a less twisted macroscopic structure.

The peak current densities are proportional to the scan rate as expected for an immobilized electroactive polymer. Between 0.0 and 0.9 V, the films can be cycled repeatedly between their conducting (oxidized) and insulating (neutral) states without significant decomposition of the materials, indicating a high electrochemical stability of the polymer.

It should be noted that no evidence of a poly(**IF**) n-doping process has been found upon cathodic polarization up to −2.5 V.

Polymer physicochemical study

Infrared absorption spectra. To elucidate the structure of poly(**IF**) *ex situ* FTIR spectroscopy was performed. **IF** or p-doped poly(**IF**) were mixed in KBr and the spectra were

Published on 23 April 2008 on http://pubs.rsc.org | doi:10.1039/B719467F
Downloaded by University of Belgrade on 01 January 2013

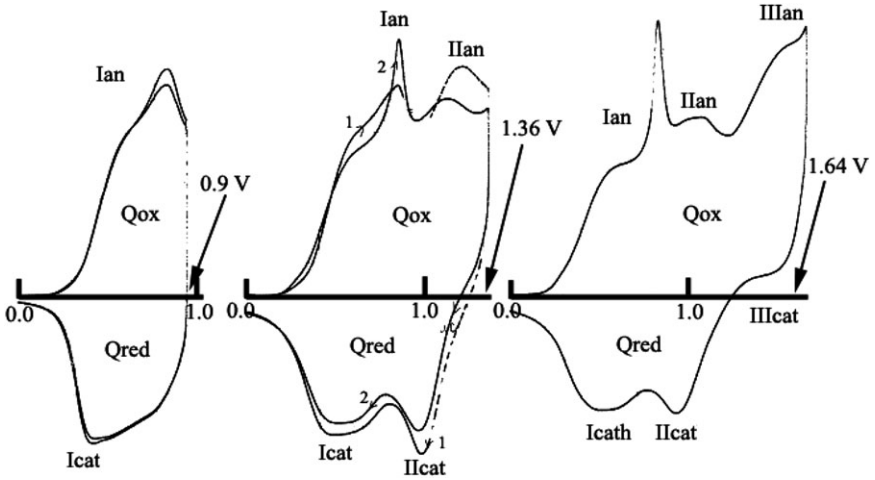

Fig. 2 Cyclic voltammetry in CH_2Cl_2 (Bu_4NPF_6 0.2 M). Working electrode: Pt disk (diameter 1 mm) modified by the deposit of poly(**IF**) prepared after the CV shown in Fig. 1(C). Sweep-rate: 100 mV s^{-1}.

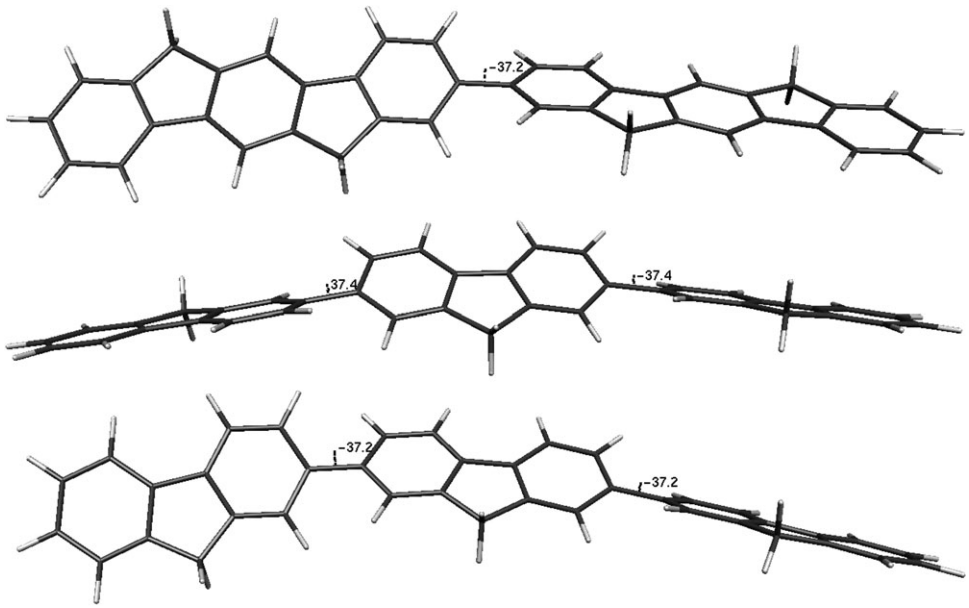

Fig. 3 Optimized geometry (Gaussian03, B3LYP/6-31G*) of one isomer of di-**IF** (top) and of two rotamers of tri-**F** (sheet-like at the centre and helical-like at the bottom), showing the value of the dihedral angles between the monomeric units.

recorded by diffuse reflection. The FTIR spectra of poly(**IF**) and **IF** are shown in Fig. 4.

Comparison of the polymer spectrum with that of the monomer shows the conservation of the monomer unit in the polymer chain as we already observed for other conjugated polymers.[31,32] The large vibration band of PF_6^- (860 cm^{-1}) in the poly(**IF**) spectrum strongly suggests that the polymer is in its p-doped form (namely, the positive charge of the electrodeposited polymer is balanced by the hexafluorophosphate anion of the electrolyte).

UV-Vis absorption spectra

Comparison of the monomer and polymer absorption spectra. Fig. 5 shows the UV-Vis spectra of **IF** in solution and of poly(**IF**) deposited on an indium tin oxide (ITO) electrode, both spectra recorded in CH_2Cl_2. **IF** shows a strong absorption between 300 and 360 nm with an absorption band edge at 345 nm. Poly(**IF**) was deposited during CVs on an ITO glass electrode and the electrodeposition was stopped when the deposit was in its neutral state (0.0 V). The poly(**IF**) film presents a large absorption band (between 275 and 500 nm), with an edge at 467 nm bathochromically shifted of 120 nm with respect to **IF**. This large absorption band can be assigned to the π–π^* transition.

Compared to the absorption edge of the UV-Vis spectrum of electrochemically prepared poly(**F**), *i.e.* 400 nm,[33] poly(**IF**) presents a bathochromic shift of 67 nm. As a higher absorption wavelength correlates with a longer conjugation length, UV-Vis spectroscopy confirmed the higher conjugation of poly(**IF**) with respect to poly(**F**). This feature is assigned to the increased rigidity of the poly(**IF**) backbone. The UV-Vis

 This journal is © The Royal Society of Chemistry and the Centre National de la Recherche Scientifique 2008

Published on 23 April 2008 on http://pubs.rsc.org | doi:10.1039/B719467F
Downloaded by University of Belgrade on 01 January 2013

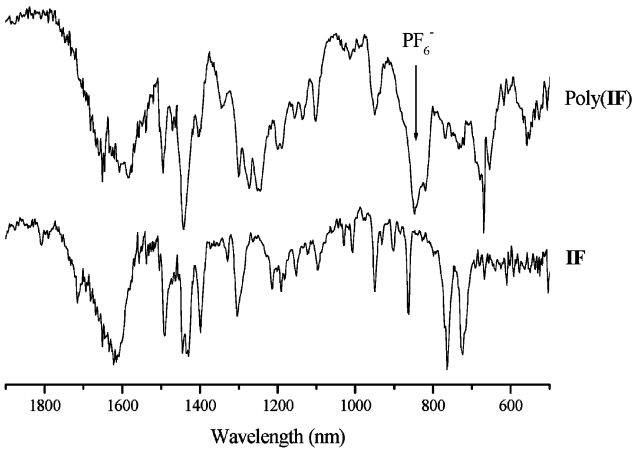

Fig. 4 FT-IR spectra of **IF** and of p-doped poly(**IF**).

spectrum of the electrochemically prepared poly(**IF**) appears to be similar to that of a chemically prepared poly(9,9-dioctylindenofluorene) (absorption edge, *ca.* 434 nm[25]). This points to a similar conjugation length in both materials (*i.e.* across five to six monomeric units).

Comparison of the monomer radical-cation and p-doped polymer absorption spectra. In order to further investigate the electronic properties of poly(**IF**), electrochemical oxidation of **IF** and poly(**IF**) were performed, monitoring the changes in their UV-Vis absorption spectra (Fig. 6). In the range of 400–1000 nm, where no absorption bands are detected for **IF** (Fig. 5), the anodic generation of $\mathbf{IF}^{\bullet+}$ (by oxidation of **IF** solution between 0.0 to 2.0 V) leads to the appearance of new bands with maxima at 410, 432, 446 and 842 nm (Fig. 6(A)). The regular increase of the absorption bands when oxidising the **IF** solution between 0.75 to 1.4 V shows the high stability of $\mathbf{IF}^{\bullet+}$ species. When oxidation is carried out at potential values higher than 1.4 V, a new absorption band appears with a maximum at 665 nm (not shown) corresponding to the formation of higher oxidation states of **IF** (bipolaron, trication-radicals). Compared with the fluorene radical-cation spectrum with maxima of 398, 467 and 678 nm,[34] $\mathbf{IF}^{\bullet+}$ absorption bands are all shifted to higher values demonstrating a larger delocalization of the polaron on a more extended aromatic structure.

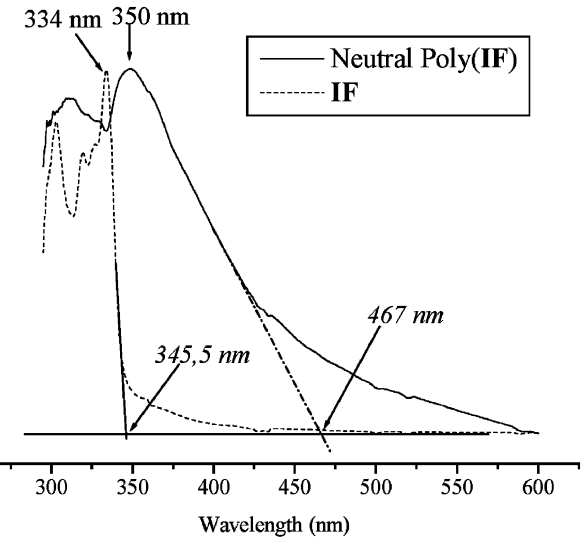

Fig. 5 Absorption spectra of **IF** recorded in solution and of neutral poly(**IF**) deposited on an ITO transparent glass electrode, both spectra are recorded in CH_2Cl_2.

The evolution of the poly(**IF**) absorption spectrum during its p-doping process is presented in Fig. 6(B). Poly(**IF**) was deposited on a platinum grid during anodic oxidation of a solution of **IF**. The modified platinum grid was then introduced into a specific cell allowing the *in situ* spectroelectrochemical study of the deposit by a gradual polarization of the electrode between 0.0 and 0.9 V and the recording of the UV spectrum at each potential step. The optical reference was the electrode modified by the deposit in its neutral state, so the decrease of the neutral polymer main absorption band (π–π* transition) appears negative in the 300–350 nm range. All the new absorption bands increasing in the 400–1300 nm range arise from the polymer in its p-doped form. The UV-Vis spectrum modification begins at 0.3 V with the appearance of several bands between 400 and 1300 nm. these bands show a regular increase when increasing the potential up to 0.9 V. The main bands have maxima at 451, 607, 669, 727 and 1047 nm corresponding to polaron and bipolaron generation. When compared to $\mathbf{IF}^{\bullet+}$, the spectrum of p-doped poly(**IF**) shows bathochromatically shifted absorption bands due to charge delocalization on a more extended aromatic structure.

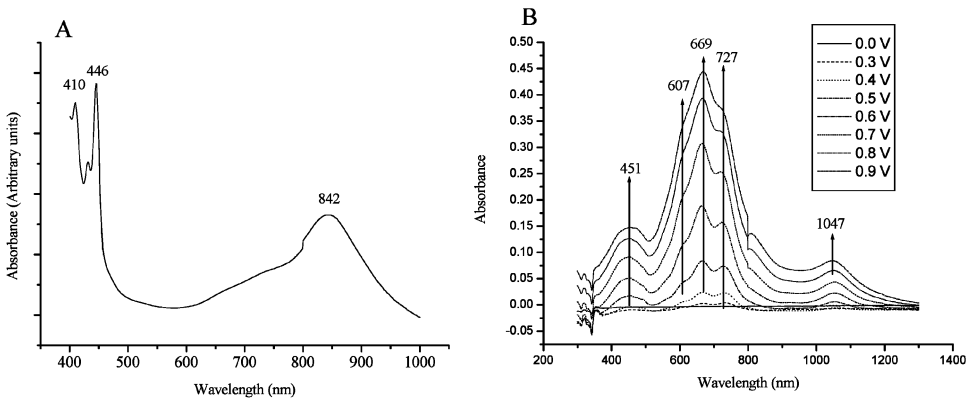

Fig. 6 Absorption spectra of (A) $\mathbf{IF}^{\bullet+}$ and (B) poly(**IF**) during its p-doping process.

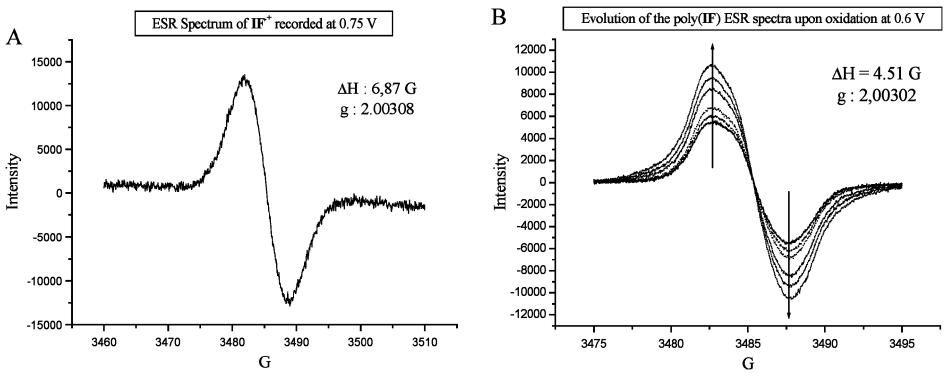

Fig. 7 ESR spectra of (A) $\mathbf{IF}^{\bullet+}$ and (B) poly(**IF**) during the p-doping process at 0.6 V.

Published on 23 April 2008 on http://pubs.rsc.org | doi:10.1039/B719467F
Downloaded by University of Belgrade on 01 January 2013

ESR spectra

Formation of the **IF** radical cation was also monitored by recording *in situ* the ESR spectrum of a solution containing **IF** during electrolysis at different potential values (from 0.75 to 1.1 V). Upon oxidation at 0.75 V, a broad singlet (ΔH_{pp} = 6.87 G, g = 2.00308) appeared, indicating the formation of **IF** radical cations (Fig. 7(A)). This ESR signal is broader than that of the fluorene radical cation[35] indicating a higher mobility of the unpaired electron on the larger molecule.

A poly(**IF**) modified electrode was prepared according to the same procedure at higher oxidation potential. Complete reduction of this electrode at 0.0 V was not possible, as a remaining ESR signal was always detected. This broader signal cannot be assigned to $\mathbf{IF}^{\bullet+}$ because this species is not stable at this potential. The p-doping/undoping process of the poly(**IF**) was recorded at 0.6 V. At this potential the dissolved **IF** is not oxidized in $\mathbf{IF}^{\bullet+}$ and the ESR spectra corresponds only to the charged species in the polymer. As observed in Fig. 6(B), starting from 0.0 V (reduction potential), we observed a broad ESR line indicating that even at such low potentials, unpaired electrons are present in the non-totally reduced polymer. When switching the potential from 0.0 to 0.6 V, we observed a gradual increase of the signal amplitude directly associated with the increase of paramagnetic species in the polymer upon the p-doping process. The g-factors, for $\mathbf{IF}^{\bullet+}$ (in solution) and for poly(**IF**) (in the thin film) are close to the free electron value of 2.0023 indicating the polaronic nature of the charge in **IF** and in poly(**IF**). The reversibility of the p-doping process allowed the initial ESR spectrum of poly(**IF**), after reduction at 0.0 V, to be obtained. The ESR studies confirm the spectroelectrochemical results concerning the stability of the radical-cation (polaron) in the monomer and the polymer.

Proposition of a mechanism for the electrodeposition process

The electrochemical and physicochemical studies discussed above and the literature data on fluorene electropolymerization and chemically synthesized poly(**IF**) lead us to propose, in Scheme 3, a mechanism for poly(**IF**) electrodeposition process.

Oxidation of **IF** leads in a first oxidation step E^1 to the formation of a stable radical cation $\mathbf{IF}^{\bullet+}$, but no polymerization occurs at this stage. When oxidation is pursued to potential values higher than E^2, more than two electrons are used and polymerization through carbon–carbon coupling between **IF** units is observed. The electrode is then covered by a p-doped poly(**IF**) deposit. Reduction of the polymer at 0.0 V leads to a neutral polymer which can be reversibly p-doped between 0.35 and 1.25 V. At higher oxidation potential, overoxidation of the polymeric matrix may occur leading to a gradually less electroactive material.

Cyclic voltammetry shows that the **IF** radical cation is stable and thus is not involved in the coupling process. Moreover, the second and third electron are abstracted from $\mathbf{IF}^{\bullet+}$ at very similar potentials. Theoretical calculations on the **IF** dication show that the singlet state is 0.92 eV more stable than the triplet state, so that it is unlikely that the electropolymerisation occurs in the dicationic state (considering a radical coupling mechanism). It is then likely that the coupling process occurs between two radical trications $\mathbf{IF}^{3\bullet+}$. Interestingly, the calculated nature of the singly occupied molecular orbital of highest energy has a strong p–π character on carbon 2 and 8 for the quadruplet state (the convergence failed on the **IF** trication doublet state). This supports the involvement of these two specific atoms in the coupling process. In addition, it has been reported that aromatic electrophilic substitution on the **IF** backbone also leads to substitution at the C2 and C8 carbon atoms.[25]

4 Conclusion

The electrochemical oxidation of indenofluorene in CH_2Cl_2–Bu_4NPF_6 0.2 M caused the formation of insoluble electroactive deposits on the working electrode surface. The deposit has a high electroactivity over a rather large potential range (0.35–1.25 V).

The mechanism and structure of the resulting polymer were proposed with the help of CV, theoretical calculations, FTIR, ESR and UV-Vis techniques. The polymer formation proceeds by a carbon–carbon coupling involving the 2 and 8 carbon atoms of the **IF** core (Scheme 3). Several substituted poly(**IF**) have been studied in the last ten years in order to estimate their potential for optoelectronic applications. However this is, to the best of our knowledge, the first example of an electrochemical synthesis of poly(**IF**). Such polymerization allows the low yield electropolymerization process observed during the anodic oxidation of class II substituted **DSF-IF** derivatives to be rationalized (Scheme 1).

 This journal is © The Royal Society of Chemistry and the Centre National de la Recherche Scientifique 2008

Published on 23 April 2008 on http://pubs.rsc.org | doi:10.1039/B719467F
Downloaded by University of Belgrade on 01 January 2013

Experimental

Chemicals

Dichloromethane with less than 100 ppm of water (ref. SDS 02910E21) was used without purification. Tetrabutylammonium hexafluorophosphate from Fluka was used without purification. Aluminium oxide was obtained from Woëlm, activated by heating at 300 °C under vacuum for 12 h and used at once under argon pressure.

Monomer synthesis

IF was prepared in a four-step synthesis[9] adapted from the procedure reported by Wang and co-workers.[36]

Electrochemical techniques

All electrochemical experiments were performed using a Pt disk electrode (diameter 1 mm). The counter electrode was a vitreous carbon rod and the reference electrode was a silver wire in a 0.1 M $AgNO_3$ solution in CH_3CN. Ferrocene was added to the electrolyte solution at the end of a series of experiments. The ferrocene/ferrocenium (Fc/Fc^+) couple served as internal standard and all reported potentials are referred to its reversible formal potential. All electrochemical investigations were conducted under argon atmosphere. Activated Al_2O_3 was added to the electrolytic solution to remove traces of moisture. The three-electrode cell was connected to a PAR Model 173 potentiostat monitored with a PAR Model 175 signal generator and a PAR Model 179 signal coulometer. The cyclic voltammetry curves were recorded on an XY SEFRAM-type TGM 164.

Polymer analysis

IR spectra were recorded using a spectrophotometer IR-FT from Nicolet model 205 by diffuse reflectance through the monomer or polymer mixed with KBr.

Liquid and solid UV-Vis spectra were recorded on a JASCO-V570 spectrophotometer. For spectroelectrochemical measurements in solution, the anode was a platinum grid. For solid UV-Vis studies, the polymer was deposited on ITO electrode or on platinum grid.

ESR spectra were recorded on a Bruker EMX-8/2.7 (X-band) spectrometer. The cation radicals were generated *in-situ* in a home-made three-electrode specific cell connected to a potentiostat. The lower part of the cell consists of a classical quartz tube used for ESR spectroscopy. Approximately 0.5 ml of electrolytic solution was introduced in the cell. The working electrode was a platinum wire at which the radical cations and/or the polymer were generated.

Computational details

Full geometry optimization with Density functional theory (DFT)[37,38] calculations were performed with the hybrid Becke-3 parameter exchange[39–41] functional and the Lee-Yang-Parr non-local correlation functional[42] (B3LYP or UB3LYP) implemented in the Gaussian 03 (Revision D.02) program suite[43] using the 6-31G* basis set[44] and the default convergence criterion implemented in the program. The figures were generated with MOLEKEL 4.3.[45]

Acknowledgements

The authors acknowledge financial support from the CNRS UMR 6226 Sciences Chimiques de Rennes and Thibaut Roux for his help in quartz microbalance measurements and the CINES (Centre Informatique National de l'Enseignement Supérieur, Montpellier) for computing time.

References

1. K. Müllen and U. Sherf, in *Organic Light-Emitting Devices: Synthesis, Properties and Applications*, Wiley-VCH, Weinheim, 2006.
2. A. C. Grimsdale and K. Müllen, *Macromol. Rapid Commun.*, 2007, **28**, 1676.
3. V. N. Bliznyuk, S. A. Carter, J. C. Scott, G. Klärner, R. D. Miller and D. C. Miller, *Macromolecules*, 1999, **32**, 361.
4. J.-I. Lee, G. Klaerner and R. D. Miller, *Chem. Mater.*, 1999, **11**, 1083.
5. U. Scherf and E. W. List, *Adv. Mater.*, 2002, **14**, 477.
6. E. W. J. List, R. Guentner, P. Scanducci de Freitas and U. Scherf, *Adv. Mater.*, 2002, **14**, 374.
7. J. M. Lupton, M. R. Craig and E. W. Meijer, *Appl. Phys. Lett.*, 2002, **80**, 4489.
8. D. Horhant, J. J. Liang, M. Virboul, C. Poriel, G. Alcaraz and J. Rault-Berthelot, *Org. Lett.*, 2006, **8**, 257.
9. C. Poriel, J.-J. Liang, J. Rault-Berthelot, F. Barrière, N. Cocherel, A. M. Z. Slawin, D. Horhant, M. Virboul, G. Alcaraz, N. Audebrand, L. Vignau, N. Huby, G. Wantz and L. Hirsch, *Chem.–Eur. J.*, 2007, **13**, 10055.
10. J. Jacob, J. Zhang, A. C. Grimsdale, K. Müllen, M. Gaal and E. J. W. List, *Macromolecules*, 2003, **36**, 8240.
11. R. Pudzich, T. Fuhrmann-Lieker and J. Salbeck, *Adv. Polym. Sci.*, 2006, **199**, 83.
12. T. P. I. Saragi, T. Spehr, A. Siebert, T. Fuhrmann-Lieker and J. Salbeck, *Chem. Rev.*, 2007, **107**, 1011.
13. J. Rault-Berthelot and J. Simonet, *J. Electroanal. Chem.*, 1985, **182**, 187.
14. J. Rault-Berthelot and J. Simonet, *New J. Chem.*, 1986, **10**, 169.
15. J. Rault-Berthelot, L. Angely, J. Delaunay and J. Simonet, *New J. Chem.*, 1987, **11**, 487.
16. J. Rault-Berthelot, M. M. Granger and L. Mattiello, *Synth. Met.*, 1998, **97**, 211.
17. As recently reported, no polymerization occurs below this potential. C. Poriel, J. Rault-Berthelot, F. Barrière and A. M. Z. Slawin, *Org. Lett.*, 2008, **10**, 373.
18. M. Samoc, A. Samoc, B. Luther-Davies and U. Sherf, *Synth. Met.*, 1997, **87**, 197.
19. M. Rumi, G. Zerbi, U. Sherf and H. Reisch, *Chem. Phys. Lett.*, 1997, **273**, 429.
20. H. A. Reisch and U. Sherf, *Synth. Met.*, 1999, **101**, 128.
21. H. Reisch, U. Wiesler, U. Sherf and N. Tuytuylkov, *Macromolecules*, 1996, **29**, 8204.
22. C. Xia and R. C. Advincula, *Macromolecules*, 2001, **34**, 6922.
23. C. Silva, M. A. Stevens, D. M. Russel, S. Setayesh, K. Müllen and R. H. Friend, *Synth. Met.*, 2001, **116**, 9.
24. C. Silva, D. M. Russel, M. A. Stevens, J. D. Mackenzie, S. Setayesh, K. Müllen and R. H. Friend, *Chem. Phys. Lett.*, 2000, **319**, 494.
25. S. Setayesh, D. Marsitzky, U. Sherf and K. Müllen, *C. R. Acac. Sci. Paris*, 2000, 471t. 1, Série IV.
26. S. Setayesh, D. Marsitzky and K. Müllen, *Macromolecules*, 2000, **33**, 2016.
27. L. M. Herz, C. Silva, R. T. Phillips, S. Setayesh and K. Müllen, *Chem. Phys. Lett.*, 2001, **347**, 318.
28. F. Laquai, P. E. Keivanidis, S. Baluschev, J. Jacob, K. Müllen and G. Wegner, *Appl. Phys. Lett.*, 2005, **87**, 261917.
29. G. Sauerbrey, *Z. Phys.*, 1959, **155**, 206.

View Article Online

30. P. Hapiot, C. Lagrost, F. LeFloch, E. Raoult and J. Rault-Berthelot, *Chem. Mater.*, 2005, **8**, 2003.
31. C. Poriel, Y. Ferrand, P. Le Maux, C. Paul, J. Rault-Berthelot and G. Simonneaux, *Chem. Commun.*, 2003, 2308.
32. I. Silaghi-Dumitrescu, J. Escudie, G. Cretiu-Nemes, E. Raoult and J. Rault-Berthelot, *Synth. Met.*, 2005, **151**, 114.
33. J. Rault-Berthelot, V. Questaigne, J. Simonet and G. Peslerbe, *New J. Chem.*, 1989, **13**, 45.
34. See the 2,7-(*t*-Bu)$_2$-fluorene radical cation UV-Vis spectrum in the ESI†.
35. See the 2,7-(*t*-Bu)$_2$-fluorene radical cation ESR spectrum in the ESI†.
36. S. Merlet, M. Birau and Z. Y. Wang, *Org. Lett.*, 2002, **4**, 2157.
37. P. Hohenberg and W. Kohn, *Phys. Rev.*, 1964, **136**, B864.
38. R. G. Parr and W. Yang, in *Density-Functional Theory of Atoms and Molecules*, Oxford University Press, Oxford, 1989.
39. A. D. Becke, *Phys. Rev. A*, 1988, **38**, 3098.
40. A. D. Becke, *J. Chem. Phys.*, 1993, **98**, 1372.
41. A. D. Becke, *J. Chem. Phys.*, 1993, **98**, 5648.
42. C. Lee, W. Yang and R. G. Parr, *Phys. Rev. B*, 1988, **37**, 785.
43. M. J. Frisch, G. W. Trucks, H. B. Schlegel, G. E. Scuseria, M. A. Robb, J. R. Cheeseman, J. A. Montgomery Jr, T. Vreven, K. N. Kudin, J. C. Burant, J. M. Millam, S. S. Iyengar, J. Tomasi, V. Barone, B. Mennucci, M. Cossi, G. Scalmani, N. Rega, G. A. Petersson, H. Nakatsuji, M. Hada, M. Ehara, K. Toyota, R. Fukuda, J. Hasegawa, M. Ishida, T. Nakajima, Y. Honda, O. Kitao, H. Nakai, M. Klene, X. Li, J. E. Knox, H. P. Hratchian, J. B. Cross, V. Bakken, C. Adamo, J. Jaramillo, R. Gomperts, R. E. Stratmann, O. Yazyev, A. J. Austin, R. Cammi, C. Pomelli, J. W. Ochterski, P. Y. Ayala, K. Morokuma, G. A. Voth, P. Salvador, J. J. Dannenberg, V. G. Zakrzewski, S. Dapprich, A. D. Daniels, M. C. Strain, O. Farkas, D. K. Malick, A. D. Rabuck, K. Raghavachari, J. B. Foresman, J. V. Ortiz, Q. Cui, A. G. Baboul, S. Clifford, J. Cioslowski, B. B. Stefanov, G. Liu, A. Liashenko, P. Piskorz, I. Komaromi, R. L. Martin, D. J. Fox, T. Keith, M. A. Al-Laham, C. Y. Peng, A. Nanayakkara, M. Challacombe, P. M. W. Gill, B. Johnson, W. Chen, M. W. Wong, C. Gonzalez and J. A. Pople, *Gaussian 03 (Revision D.02)*, Gaussian Inc., Wallingford, CT, 2004.
44. P. C. Hariharan and J. A. Pople, *Chem. Phys. Lett.*, 1972, **16**, 217.
45. *MOLEKEL 4.3*, P. Flükiger, H. P. Lüthi, S. Portmann and J. Weber, Swiss National Supercomputing Centre, CSCS, Manno, Switzerland, 2000.

Published on 23 April 2008 on http://pubs.rsc.org | doi:10.1039/B719467F
Downloaded by University of Belgrade on 01 January 2013

 This journal is © The Royal Society of Chemistry and the Centre National de la Recherche Scientifique 2008